

# BCS-like Bogoliubov Quasiparticles in High- $T_c$ Superconductors Observed by Angle-Resolved Photoemission Spectroscopy

H. Matsui<sup>1</sup>, T. Sato<sup>1</sup>, T. Takahashi<sup>1</sup>, S.-C. Wang<sup>2</sup>, H.-B. Yang<sup>2</sup>, H. Ding<sup>2</sup>, T. Fujii<sup>3,\*</sup>, T. Watanabe<sup>4,†</sup>, and A. Matsuda<sup>4</sup>

(1)Department of Physics, Tohoku University, Sendai 980-8578, Japan

(2)Department of Physics, Boston College, Chestnut Hill, MA 02467, USA

(3)Department of Applied Physics, Faculty of Science, Science University of Tokyo, Tokyo 162-8601, Japan

(4)NTT Basic Research Laboratories, Atsugi 243-0198, Japan

We performed high-resolution angle-resolved photoemission spectroscopy on triple-layered high- $T_c$  cuprate  $\text{Bi}_2\text{Sr}_2\text{Ca}_2\text{Cu}_3\text{O}_{10+\delta}$ . We have observed the full energy dispersion (electron and hole branches) of Bogoliubov quasiparticles and determined the coherence factors above and below  $E_F$  as a function of momentum from the spectral intensity as well as from the energy dispersion based on BCS theory. The good quantitative agreement between the experiment and the theoretical prediction suggests the basic validity of BCS formalism in describing the superconducting state of cuprates.

PACS numbers: 74.72.Hs, 74.20Fg, 79.60.Bm

It is well known that BCS (Bardeen, Cooper, and Schrieffer) theory [1] explains many of fundamental thermodynamic, transport and magnetic properties of superconductors by introducing a simple picture that two electrons with opposite momenta and spins near the Fermi surface form a pair (Cooper pair) in the superconducting state. In the language of Fermi liquids [2], the quasiparticles (QPs) of the Cooper pairs are called Bogoliubov quasiparticles (BQPs) [3] which are defined as excitation of a single electron “dressed” with an attractive interaction between paired electrons. The BQPs play an essential role in characterizing the superconducting state via quantities such as the superconducting gap and its symmetry. Despite the excellent description of the BQPs in BCS theory, there has been no direct experimental observation of the predicted full energy dispersion (electron and hole branches) of BQPs, although the pairing of electrons is evidenced by ac Josephson-junction experiment [4]. For high- $T_c$  cuprates, the direct observation of the BQPs is even more significant, since many microscopic ideas of BCS theory have been seriously challenged. Since the BQPs are a natural consequence of the starting Hamiltonian including the two-body attractive interaction assumed by BCS theory [1], the existence of BQPs would prove the validity of the basic BCS description of the superconducting state in the cuprates.

In this Letter, we report the direct observation of BQPs in triple-layered high- $T_c$  cuprate  $\text{Bi}_2\text{Sr}_2\text{Ca}_2\text{Cu}_3\text{O}_{10+\delta}$  by angle-resolved photoemission spectroscopy (ARPES). By using ultrahigh resolution in energy and momentum, we have succeeded in directly observing the full energy dispersion (electron and hole branches) of BQPs below and above the Fermi level ( $E_F$ ). We have determined experimentally the coherence factors as a function of momentum from ARPES intensity and compared the result with the prediction from BCS theory to investigate the basic

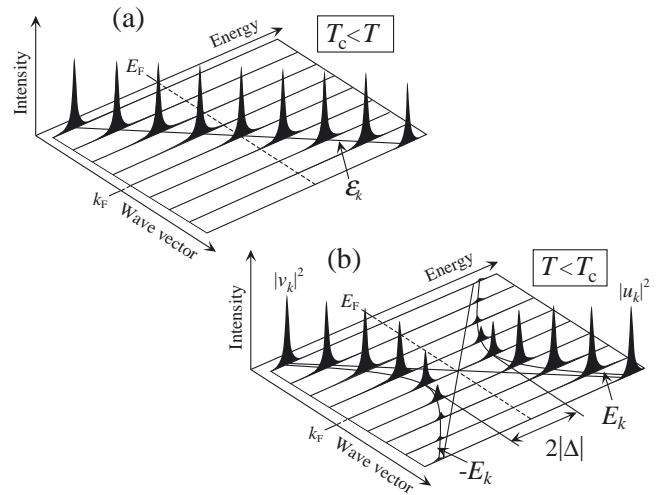


FIG. 1. Schematic diagram of the formation process of a Bogoliubov-quasiparticle (BQP) band. In the normal state above  $T_c$  (a), the electron band has an equal weight at any momentum, while in the superconducting state below  $T_c$  (b), particle-hole mixing (mixing of electron and hole bands) takes place due to the pairing, leading to opening of a superconducting gap as well as a transfer of weight between the electron and hole bands.

validity of the theory in high- $T_c$  cuprates.

High-quality single crystals of  $\text{Bi}_2\text{Sr}_2\text{Ca}_2\text{Cu}_3\text{O}_{10+\delta}$  (Bi2223, overdoped,  $T_c=108$  K) were grown by the traveling solvent floating zone method [5]. ARPES measurements were performed using a GAMMADATA-SCIENTIA SES-200 spectrometer with 22 eV photons at the undulator 4m-NIM beamline at Synchrotron Radiation Center in Wisconsin. The energy and angular (momentum) resolutions were set at 11 meV and  $0.2^\circ$  ( $0.007\text{\AA}^{-1}$ ), respectively. A clean fresh surface of sample was obtained by *in-situ* cleaving along the (001) plane.

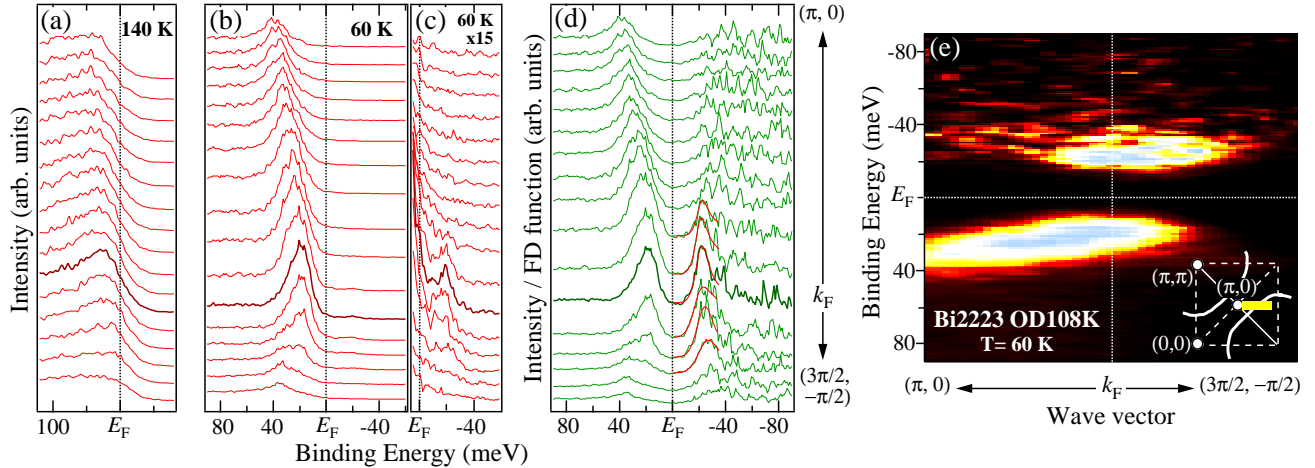


FIG. 2. (a) ARPES spectra of Bi2223 in the normal state (140 K) measured along a yellow line in the Brillouin zone shown in the inset in (e). Spectrum at  $k_F$  is indicated by a dark red line. (b) ARPES spectra taken under the same condition as in (a) but at the superconducting state (60 K). (c) Same as (b) in an expanded intensity scale above  $E_F$ . (d) ARPES spectra in (b) divided by the FD function at 60 K convoluted with a Gaussian reflecting the instrumental resolution. Spectrum at  $k_F$  is indicated by a dark green line. Red lines are fitting curves for unoccupied states using a Lorentzian with energy-dependent broadening factor. Fittings are restricted to the spectra of which peak positions are located within  $5k_B T$  from  $E_F$ . (e) Intensity plot of normalized ARPES spectra in (d) as a function of binding energy and wave vector. Momentum region is the same in (a)-(d).

The Fermi level ( $E_F$ ) of the sample was referenced to that of a gold film evaporated onto the sample substrate.

Figure 1 shows a schematic comparison of spectra between the superconducting BQPs and the normal-state QPs. In the normal state [Fig. 1(a)], one-electron like QPs disperse across  $E_F$  with an equal spectral weight, defining the Fermi vector ( $k_F$ ) at  $E_F$ . In the superconducting state [Fig. 1(b)], the BQPs split the single band into two dispersing branches below and above  $E_F$ . The BQPs exhibit several characteristic features: (i) the dispersion of two branches is symmetric with respect to  $E_F$ ; (ii) the minimum separation at  $k_F$  defines the superconducting energy gap ( $2\Delta$ ); (iii) both the dispersions below and above  $E_F$  show bending-back behavior at  $k_F$  due to the particle-hole mixing; (iv) the spectral weight of the two branches differs, and changes with the wave vector  $k$ ; however, (v) the combining weight of the two branches is always constant at any  $k$ .

Figures 2(a) and 2(b) show the ARPES spectra of Bi2223 in the normal and superconducting states, respectively, measured along the direction in the Brillouin zone shown in the inset in Fig. 2(e). We have surveyed many areas in the Brillouin zone and confirmed that the intensity of Umklapp bands is very weak and they do not contaminate the main-band dispersion in this momentum region. While we see a broad peak dispersing across  $E_F$  in the normal state, we clearly observe a sharp coherent peak in the superconducting state [6]. As  $k$  is changed from  $(\pi, 0)$  to  $(3\pi/2, -\pi/2)$ , the coherent peak gradually disperses toward  $E_F$ , showing a minimum energy gap at  $k_F$  [dark red line in Fig. 2(b)], and then disperses back

to the higher binding energy while rapidly reducing its intensity. These behaviors are consistent with the band dispersion below  $E_F$  shown in Fig. 1(b) as well as with a previous ARPES result on  $\text{Bi}_2\text{Sr}_2\text{CaCu}_2\text{O}_{8+\delta}$  (Bi2212) [9]. More importantly, we find additional weak but discernible structures about 20 meV above  $E_F$  in the spectra, which are more clearly seen in Fig. 2(c). This new structure shows a clear momentum dependence with a stronger intensity in the region of  $|k| > |k_F|$ , opposite to the behavior of the band below  $E_F$ . We ascribe these small structures to the BQP band above  $E_F$  by referring to Fig. 1(b) [10]. The considerably weak intensity of the peaks above  $E_F$  is simply due to the effect of the Fermi-Dirac (FD) function. In order to see more clearly the band dispersion above  $E_F$ , we have divided the ARPES spectra by the FD function at 60 K convoluted with the instrumental resolution [11]. The result is shown in Fig. 2(d), where we find a dispersive structure with comparable intensity above  $E_F$ , although the signal-to-noise ratio is relatively low because of the originally small ARPES intensity. It is remarked here that despite the low signal-to-noise ratio the bending-back behavior of band is also seen in the unoccupied states as in the occupied states. The dispersive feature is more clearly visualized in Fig. 2(e) by plotting the renormalized ARPES intensity as a function of momentum and energy. We observe several characteristic behaviors for the two branches: (i) the dispersive feature is almost symmetric with respect to  $E_F$  while the intensity is not; (ii) the bands have a minimum energy gap at  $k_F$ ; (iii) both bands show the bending-back effect at  $k_F$ ; (iv) the spectral intensity of the two

bands show opposite evolutions as a function of  $k$  in the vicinity of  $k_F$ . All these features qualitatively agree with the behaviors of BQPs predicted from BCS theory [Fig. 1(b)], suggesting the basic validity of the BQP concept in high- $T_c$  superconductors.

The next question is how quantitatively the observed dispersion and spectral weight agree or disagree with the predictions from BCS theory. This point is crucial in establishing the BQP concept more firmly in the cuprates. Figure 3(a) shows direct comparison between the experimental band dispersion of BQPs (same as Fig. 2(e)) and the corresponding calculated curves based on BCS theory. In BCS theory, the band dispersion of BQPs ( $E_k$ ) is expressed as  $E_k = [\epsilon_k^2 + |\Delta(k)|^2]^{1/2}$ , where  $\epsilon_k$  and  $\Delta(k)$  are the normal-state dispersion and the superconducting gap, respectively. We have determined at first  $\epsilon_k$  and  $\Delta(k)$  from the ARPES spectra at 140 and 60 K in Fig. 2, respectively, and then calculated the ‘‘theoretical’’ band dispersion of BQPs using the above equation. The normal state dispersion  $\epsilon_k$  [white solid line in Fig. 3(a)] is obtained from the peak position in ARPES spectra at 140 K [white open circles in Fig. 3(a)] by fitting them with parabolic function. The superconducting gap  $\Delta(k)$  is assumed to be the  $d_{x^2-y^2}$ -wave superconducting order parameter  $\Delta(k) = \Delta_0 |\cos(k_x) - \cos(k_y)|/2$ , where  $\Delta_0$  is determined by the peak energy of the 60-K spectrum at  $k_F$ . We find in Fig. 3(a) that the calculated dispersion well traces the strong-intensity areas of ARPES spectra, showing good agreement in the band dispersion between the experiment and the theory. To further confirm the agreement in the unoccupied states, we have fit the normalized ARPES spectra in Fig. 2(d) with a Lorentzian and show the peak positions in Fig. 3(a). The peak positions are found to be well on the calculated curve, showing quantitatively good agreement between the experiment and the calculation.

To further study the validity of the BQP concept, we have determined the coherence factors above and below  $E_F$ ,  $|u_k|^2$  and  $|v_k|^2$ , by using the following two independent methods and compared them with each other. The coherence factors are defined as the relative intensity of BQP bands above and below  $E_F$ , which directly correspond to the normalized ARPES spectral intensity in the superconducting state. On the other hand, according to BCS theory, the coherence factors can be also calculated from the energy dispersions of the normal-state QP and the superconducting BQP bands in the following way:

$$|u_k|^2 = 1 - |v_k|^2 = \frac{1}{2} \left( 1 + \frac{\epsilon_k}{E_k} \right) \quad (1)$$

where  $\epsilon_k$  and  $E_k$  are the energy of the normal QP and BQP bands, respectively [1].

For the first method, we have determined  $|u_k|^2$  and  $|v_k|^2$  by fitting the original ARPES spectra in Fig. 2(b) by the following equation,

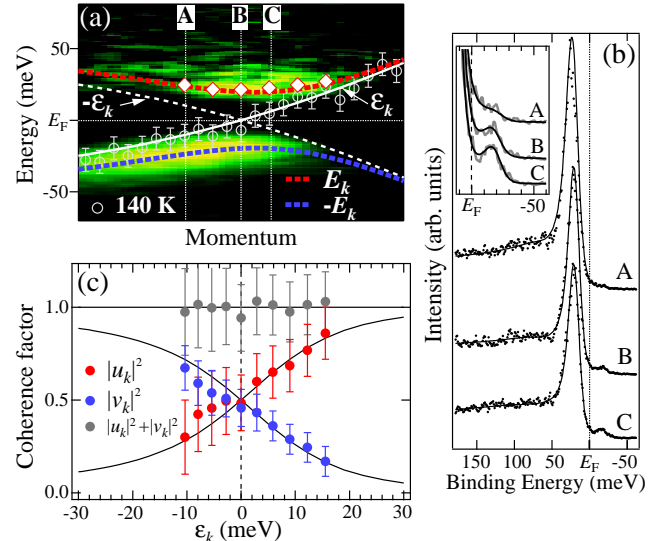


FIG. 3. (a) Comparison of the ARPES intensity plot (same as Fig. 2(e)) with the calculated BQP band dispersions based on BCS theory (red and blue dashed lines). Calculation has been performed using the BCS formula  $E_k = [\epsilon_k^2 + |\Delta(k)|^2]^{1/2}$ , where  $\epsilon_k$  (white solid line) has been determined by fitting the spectral peak positions at 140 K (white open circles) using parabolic function. The corresponding hole band ( $-\epsilon_k$ ) is also shown by a white dashed line. Peak positions of Lorentzian to fit the normalized ARPES spectra in the unoccupied states (Fig. 2(d)) are shown by white filled squares for comparison. (b) ARPES spectra (dots) measured at three representative points in the Brillouin zone shown in (a) (points A, B, and C), together with the fitting curves (solid lines) to obtain the coherence factors ( $|u_k|^2$  and  $|v_k|^2$ ). The inset shows expansion near  $E_F$ . (c) Coherence factors as a function of  $\epsilon_k$  determined from ARPES intensity (red and blue solid circles), compared with those derived from ARPES dispersion using BCS formula (solid lines). Sum of two coherence factors ( $|u_k|^2 + |v_k|^2$ ) obtained by ARPES intensity is shown by gray solid circles.

$$I(k, \omega) =$$

$$I_0(k) \int d\omega' \{A_{BCS}(k, \omega') + A_{inc}(k, \omega')\} f(\omega') R(\omega - \omega') \quad (2)$$

where  $I_0(k)$  is a prefactor which includes some kinematical factors and the dipole matrix-element.  $A_{BCS}(k, \omega)$  is the BCS spectral function expressed as,

$$A_{BCS}(k, \omega) = \frac{1}{\pi} \left\{ \frac{|u_k|^2 \Gamma}{(\omega - E_k)^2 + \Gamma^2} + \frac{|v_k|^2 \Gamma}{(\omega + E_k)^2 + \Gamma^2} \right\} \quad (3)$$

where  $\Gamma$  is a linewidth broadening due to the finite lifetime of photoholes.  $A_{inc}(k, \omega)$  in Eq. (2) is an empirical function representing the incoherent background [12],  $f(\omega)$  is the FD function, and  $R(\omega)$  is the Gaussian resolution function. To remove the effect of  $I_0(k)$ , we have divided the spectral intensity of the superconducting state (60 K) with the integrated normal-state (140 K) spectral

intensity at each  $k$  point. We determine the peak weights below and above  $E_F$  at each  $k$  point by decomposing the spectrum, and then divide them by the average value of the total peak weight at each  $k$  point [15]. We define these normalized weights as  $|v_k|^2$  and  $|u_k|^2$  and show the results in Fig. 3(c). It is important to note here that  $|u_k|^2$  and  $|v_k|^2$  are determined independently without using the sum rule of  $|u_k|^2 + |v_k|^2 = 1$ . The fittings have been performed within the momentum region where reliable values for the coherence factors can be obtained [shown in Fig. 3(c)], since the reliability of fitting is considerably decreased far above  $E_F$  due to the low signal-to-noise ratio of the original ARPES spectra.

For the second method, we have calculated  $|u_k|^2$  and  $|v_k|^2$  by using Eq. (1) with  $\epsilon_k$  and  $E_k$  obtained from Fig. 3(a). In Fig. 3(c), we show the comparison of the two sets of coherence factors determined by the ARPES intensity itself and by the BCS calculation based on the band dispersions, respectively. We find a surprisingly good quantitative agreement between the two sets of coherence factors determined totally independently [16]. It is also remarked that the sum of coherence factors,  $|u_k|^2 + |v_k|^2$ , determined by the ARPES intensity is almost constant over the measured momentum region, in good agreement with the sum rule of the coherence factors predicted from BCS theory.

The sharp superconducting quasiparticle peak at  $(\pi, 0)$  in Bi-based cuprates has been widely studied in the high- $T_c$  field. The origin and its implications are still under debate. Some of its properties clearly deviate from BCS theory. For example, the leading edge of the quasiparticle peak does not reach  $E_F$  even above  $T_c$ , indicating the opening of a pseudogap [17]. Spectral weight of the quasiparticle peak increases with hole-doping and has an unusual temperature dependence [13,14]. The present ARPES study, on the other hand, by its direct experimental observation of two dispersive branches with their dispersions and coherence factors consistent with the BCS predictions, has unambiguously established the Bogoliubov-quasiparticle nature of this sharp peak. This implies that the superconducting state of the high- $T_c$  cuprate is BCS-like, so that some of the basic BCS formalism is still valid in this case, although the pairing mechanism and other exotic properties are beyond BCS theory. Thus this experimental observation provides a strong constraint in modeling the high- $T_c$  problem. Moreover, this observation opens a new way to study quasiparticles in the superconducting state by probing the branch above  $E_F$  populated by thermal or optical excitations. One particularly important application is to determine the nature of the gapped peak in the pseudogap state. This may potentially settle the debate between the precursor pairing gap and single-particle gap.

We thank T. Tohyama, K. Yamada, J. R. Engelbrecht and Z. Wang for useful discussions. This work is supported by grants from the MEXT of Japan, US NSF

DMR-0072205, and Sloan Foundation. T.S. thanks JSPS for financial support. The Synchrotron Radiation Center is supported by US NSF DMR-0084402.

\*Present address: Department of Applied Physics, Waseda University, Tokyo 169-8555, Japan

†Present address: NTT Photonics Laboratories, Atsugi 243-0198, Japan

- 
- [1] J. Bardeen, L. N. Cooper, and J. R. Schrieffer, *Phys. Rev.* **108**, 1175 (1957).
  - [2] L. D. Landau, *Sov. Phys. JETP* **3**, 920 (1957).
  - [3] N. N. Bogoliubov, *Nuovo Cimento* **7**, 794 (1958).
  - [4] R. C. Jaklevic, J. Lambe, J. E. Mercereau, and A. H. Silver, *Phys. Rev.* **140**, A1628 (1965).
  - [5] T. Fujii, T. Watanabe, and A. Matsuda, *J. Cryst. Growth* **223**, 175 (2001).
  - [6] In the present study of Bi2223, multiple bands are not clearly resolved either in the normal or in the superconducting state [7,8] in contrast to the case of Bi2212.
  - [7] D. L. Feng *et al.*, *Phys. Rev. Lett.* **88**, 107001 (2002).
  - [8] H. Matsui *et al.*, *Phys. Rev. B* **67**, 060501 (2003).
  - [9] J. C. Campuzano *et al.*, *Phys. Rev. B* **53**, R14737 (1996).
  - [10] There are several favorable conditions in Bi2223 which enable the direct observation of the unoccupied states by ARPES in contrast to other high- $T_c$  cuprates such as Bi2212: (i) The coherent peak is sharp and strong enough to survive the cutting-off effect by the FD function above  $E_F$ . (ii) Higher  $T_c$  is favorable because the spectral weight above  $E_F$  increases due to the FD-function effect. (iii) Temperature of measurement should be sufficiently lower than  $T_c$ , because the intensity of the coherent peak is substantially depressed near  $T_c$ . These conditions are better fulfilled in Bi2223 than in Bi2212.
  - [11] T. Greber, T. J. Kreutz, and J. Osterwalder, *Phys. Rev. Lett.* **79**, 4465 (1997).
  - [12] We assumed a linear background with a cutoff with respect to  $E_F$  to represent the incoherent part of the spectra, as employed in previous ARPES studies on Bi2212 [13,14].
  - [13] D. L. Feng *et al.*, *Science* **289**, 277 (2000).
  - [14] H. Ding *et al.*, *Phys. Rev. Lett.* **87**, 227001 (2001).
  - [15] We did not use the normal-state quasiparticle weight for division, because the quasiparticle weight in ARPES spectrum shows temperature dependence in cuprates [13,14].
  - [16] A slight deviation between the experimental and calculated curves in the occupied side may be due to the tri-layer splitting and/or the van Hove singularity located just below  $E_F$ .
  - [17] H. Ding *et al.*, *Nature (London)* **382**, 51 (1996).